

The Vibrational Spectroscopic (FT-IR & FT Raman, NMR, UV) study and HOMO& LUMO analysis of Phthalazine by DFT and HF Studies

C. C. Sangeetha ¹, R. Madivanane ², V. Pouchaname ³

¹Department of Physics, Manonmaniyam Sundaranar University, Tirunelveli, Tamil Nadu, India.

²Department of Physics, Bharathidasan Government College for Women, Puducherry, India.

³Department of Chemistry, Bharathidasan Government College for Women, Puducherry, India.

E.Mail : carosangee@gmail.com

Mobile number: 09994313341

Abstract : In this work the FT-IR FT-Raman, UV-Visible absorption and ¹H NMR spectra of Phthalazine were registered, assigned and analyzed. The spectra were interpreted with aid of normal coordinate analysis based on DFT/B3LYP and HF methods using standard 6-311++G(d,p) basis set. After scaling there is good agreement between the observed and the calculated frequencies. Bond lengths, angles and dipole moments for the optimized structures of Phthalazine were also calculated. The calculated first order hyperpolarizability shows that the molecule is an attractive molecule for future applications in non linear optics. The calculated Homo-Lumo energies show that charge transfer occurs within the molecule. Mullikan population analysis on atomic charges is also calculated. The study is extended to study the thermodynamic properties of Phthalazine. The ¹H nuclear magnetic resonance (NMR) chemical shifts of the molecule were calculated by the gauge independent atomic orbital (GIAO) method and compared with experimental results. UV-Vis spectrum of the compound was recorded and electronic properties were performed. Finally, the calculated results were applied to simulated infrared and Raman spectra of the title compound which show good agreement with observed spectra.

Keywords : Phthalazine, Vibrational analysis, FTIR, FT-Raman, DFT calculation, Homo-Lumo analysis, thermodynamical properties, GIAO, UV-vis spectrum, Gaussian 09.

INTRODUCTION

Phthalazine is a diazaphthalene with two adjacent N atoms. Phthalazines are examples of nitrogen heterocycles that possess exciting biological properties.[1-3].The numerous studies published on their applicability in different areas, especially as Drugs[4,5]. Phthalazines have been reported to possess, anticonvulsant, [6] cardiotoxic, [7] antimicrobial, [8] antitumor, [9-12] antihypertensive, [13,14] antithrombotic,[15] antidiabetic, [16,17] antitrypanosomal,[18] anti-inflammatory,[18-22] and vasorelaxant activities[23].Additionally, Phthalazines have recently been reported to potentially inhibit serotonin reuptake and are considered anti-depression agents.[24].This compound have wide range of applications as therapeutic agents. Phthalazine and its derivatives

possessing triazines nucleus has attracted great attention in recent years due to extensive variety of biological activity, particularly anticonvulsant activity. They are used as an intermediate in the synthesis of antimalarial drugs and its derivatives are used as antimicrobial agents. Phthalazine shows anti tumor activity. The new Phthalazine substituted urea and thiourea derivatives inhibited the hAs I AND II enzyme activity. Therefore, our results suggested that the compounds are likely to be adopted as candidates to treat Glaucoma. Amio derivatives of 2,3 -dihydrophthalazine -1,4-dione were used in the treatment of various diseases in humans, in particular ,anti inflammatory immuno correcting activity in the treatment of ulcer. The 4-Arylphthalazones bearing benzenesulfonamide is used as anti-inflammatory and anti cancer agents. Thus, owing to the industrial and biological importance extensive spectroscopic studies on Phthalazine were carried out by recording the FTIR and FT-Raman spectra, NMR and UV-Visible and subjecting them to normal coordinate analysis. Literature survey reveals that, to the best of our knowledge no HF and B3LYP level calculations of Phthalazine have been reported so far. In the present work, the experimental and theoretical FT-IR and FT-Raman spectra of Phthalazine have been studied. The HF and B3LYP level with 6-311++G (d,p) basis set have been performed to obtain the ground state optimized geometries and the vibrational wave numbers of the different normal modes as well as to predict the corresponding intensities for the different modes of the molecule. The present research work was undertaken to study the vibrational modes and also to carry out HOMO-LUMO, Polarizability, Hyper polarizability, Mullikan's charge density and thermodynamical properties for the title molecule.

2. Experimental setup and measurements:

2.1 Spectral details:

The fine sample of Phthalazine provided by the Sigma Aldrich Chemical Co.(USA), with a stated purity of greater than 98%, was used as such for the spectral measurements. At the room temperature a Fourier Transform IR spectrum of the title compound was measured in 3500-0 cm^{-1} region at a resolution of $\pm 2 \text{ cm}^{-1}$ using Bruker IFS -66V Fourier transform spectrometer. The FT-Raman spectrum of Phthalazine was recorded on the same instrument equipped with an FRA -106 FT- Raman accessory. The spectrum was recorded in the 3500-0 cm^{-1} with Nd: YAG laser operating at 200 mW power. The reported wave numbers are expected to be accurate within $\pm 2 \text{ cm}^{-1}$. ^1H nuclear magnetic resonance (NMR) (400 MHz; CDCl_3) spectra were recorded on a Bruker HC400 instrument. Chemical shifts for protons are reported in parts per million scale downfield from tetramethylsilane. NMR spectra are recorded using 2BRUKER 500 MHz AVANCE III instruments using CDCl_3 as solvent, with TMS as an internal standard. Proton (^1H) spectrum at 500 MHz is recorded at room temperature. The Ultra- violet absorption spectrum of Phthalazine, dissolved in CdCl_2 solution, was recorded in the range 200.00 to 400.00 nm using SHIMADZU UV-1601 PC, UV-1700 Series spectrometer. The

theoretically predicted FT-IR and Raman spectra at three parameter hybrid functional Lee-Yang-Parr (B3LYP) using 6-311++G(d,p) basis set level of calculations along with experimental FT-IR and FT-Raman spectra are shown in Figures.

2.2 Computational Details

Using the version of Gaussian 09 W (revision B.01) program, the DFT and HF calculations of the title compound were carried out on Intel core2 duo /2.20 GH processor. Becke-3-lee-yang-parr (B3LYP) functions were used to carry out Ab-initio analysis with the standard 6-311++G(d,p) basis sets. The normal coordinate analysis of the compound Phthalazine has been computed at the fully optimized geometry. For the simulated IR and Raman spectra pure Lorentzian band shapes with the band width of 10 cm^{-1} was employed using the Gabedit version 2.3.2. In order to improve the calculated values in agreement with the experimental values, it is necessary to scale down the calculated harmonic frequencies. Hence, the vibrational frequencies calculated at DFT level are scaled by 0.98 and at HF level the frequencies are scaled by 0.96 [25, 26]. After scaled with the scaling factor, the deviation from the experiments is less than 10 cm^{-1} with a few exceptions. The animation option of the Gauss view 05 graphical interface for Gaussian program was employed for the proper assignment of the title compound and to check whether the mode was pure or mixed. The idea of using multiple scale factors in the recent literature [28] has been adapted for this study and it minimized the deviation between the computed and the experimental frequencies. Most of the scale factors are much closer to the unity for DFT and HF studies which implies that B3LYP/6-311++G (d, p) computations yield results much closer to the experimental values. UV-Vis spectra electronic transitions vertical excitation energies, absorbance and oscillator strength were computed with TD-DFT method. Finally the Nuclear Magnetic Resonance (NMR) chemical shifts were performed using Gauge induced Atomic Orbital (GIAO) method [29,30].

Prediction of Raman intensities:

The Raman activities (S_{Ra}) calculated with GAUSSIAN 03 program [31] converted to relative Raman intensities (I_{Ra}) using the following relationship derived from the intensity theory of Raman scattering [32,33],

$$I_i = f (v_0 - v_i)^4 S_i / v_i [1 - \exp(-hc v_i / kT)]$$

Where, v_0 is the laser exciting wave number in cm^{-1} (here $v_0 = 9398.5\text{ cm}^{-1}$).

v_i vibrational wavenumber of the i^{th} normal mode. (cm^{-1})

S_i Raman scattering activity of the normal mode v_i .

f_i is a constant.(equal to 10^{12}) It is a suitably chosen common normalization factor for all peak intensities, h , k , c and T are Planck and Boltzmann constants and speed of light and temperature in Kelvin, respectively.

3. Result and Discussions:

3.1 Molecular Structure:

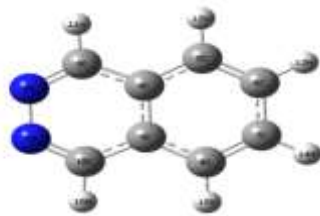


Figure 1: Optimized molecular structure of Phthalazine.

Parameters	DFT(B3LYP) 6-311++G(d,p)	HF 6-311++G(d,p)	Parameters	DFT(B3LYP) 6-311++G(d,p)	HF/6-311++G(d,p)
BOND LENGTH			DIHEDREL ANGLE (°)		
N1-N2	1.3657	1.3471	C10- N1-C2- C3	0	0
N1-C10	1.3101	1.2818	C2- N1-C10-C9	0	0
N2-C3	1.3101	1.2818	C2- N1-C10-16	180	-180
C3-C4	1.423	1.4278	N1- N2- C3-C4	0	0
C3-H11	1.0875	1.0771	N1- N2-C3-H11	-180	180
C4-C5	1.4137	1.4113	N2-C3-C4-C5	180	-180
C4-C9	1.4148	1.39	N2-C3-C4-C9	0	0
C5-C6	1.377	1.3627	H11-C3-C4,C5	0	0
C5-12H	1.0846	1.0755	H11-C3-C4-C9	180	180
C6-C7	1.4147	1.4136	C3-C4-C5-C6	180	180
C6-H13	1.084	1.0751	C3-C4-C5-H12	0	0
C7-C8	1.377	1.3627	C9-C4-C5-C6	0	0
C7-H14	1.084	1.0751	C9-C4-C5-H12	180	180
C8-C9	1.4137	1.4113	C3-C4-C9-C8	180	180
C8-H15	1.0846	1.0755	C3-C4-C9-C10	0	0
C9-C10	1.423	1.4278	C5-C4-C9-C8	0	0

C10-H16	1.0875	1.0771	C5-C4-C9-C10	-180	180
BOND ANGLE (°)			C4-C5-C6-C7	0	0
N2- N1-10C	119.5093	120.1254	C4-C5-C6-H13	180	-180
N1- N2- C3	119.5093	120.1254	H12-C5-C6-C7	180	180
N2-C3-C4	124.6255	124.0542	H12-C5-C6-H13	0	0
N2-C3-11H	115.4224	116.0187	C5-C6-C7-C8	0	0
C4- C3-H11	119.952	119.9271	C5-C6-C7-H14	180	180
C3-C4-C5	124.3686	124.1785	H13-C6-C7-C8	180	180
C3-C4-C9	115.8652	115.8205	H13-C6-C7-H14	0	0
C5-C4-C9	119.7663	120.001	C6-C7-C8-C9	0	0
C4-C5-C6	119.5889	119.3888	C6-C7-C8-H15	180	180
C4-C5-12H	119.577	119.7767	H14-C7-C8-C9	180	180
C6-C5-H12	120.834	120.8345	H14-C7-C8-H15	0	0
C5C-C6-C7	120.6448	120.6101	C7-C8-C9-C4	0	0
C5-C6-H13	120.0181	120.1084	C7-C8-C9-C10	180	180
C7-6C-H13	119.3371	119.2815	H15-C8-C9-C4	-180	180
C6-C7-C8	120.6448	120.6101	H15-C8-C9-C10	0	0
C6-C7-H14	119.3371	119.2815	C4-C9-C10- N1	0	0
C8-C7-H14	120.0181	120.1084	C4-C9-C10-H16	180	180
C7C-C8-C9	119.5889	119.3888	C8-C9-C10- N1	180	-180

C7-C8-H15	120.834	120.8345	C8-C9-C10-H16	0	0
C9-C8-H15	119.577	119.7767			
C4-C9-C8	119.7663	120.001			
C4-C9-C10	115.8652	115.8205			
C8-C9-C10	124.3686	124.1785			
N1-C10-C9	124.6255	124.0542			
N1-C10-H16	115.4224	116.0187			
C9-C10-H16	119.952	119.9271			

Table 1: Comparison of the geometrical parameters of Phthalazine from DFT and HF studies.

The general molecular structure and atom numbering of Phthalazine molecule, under investigation is represented in Figure 1. The geometry of Phthalazine under investigation possessing C₁ point group symmetry. The 42 fundamental modes of vibrations are present in Phthalazine molecule. Determining the optimized molecular structure is the first task of the computational work. The numbering schemes of the atoms were obtained from Gauss view programs[34]. The optimized structural parameters such as bond length, bond angles and dihedral angles of Phthalazine molecule are determined by B3LYP and HF level with 6-311++G (d,p) as basis set. Geometric properties of structure were calculated by B3LYP/6-311++G (d,p) and HF/6-311++G (d,p) levels of calculation and depicted in Table 1. The bond lengths of C-C are greater than C-H bond lengths. The bond lengths related to Nitrogen atoms are with the values as 1.31. The density functional calculation gives almost same bond angles. The dihedral angles of our title molecule shows that our tested molecule was planar. The optimized bond length and bond angles are slightly smaller than the experimental values. This is due to the fact that all the theoretical calculations belongs to isolated molecule were done in gaseous state and the experimental results were belongs to molecule is in solid state.

3.2 Vibrational Assignments:

The harmonic vibrational frequencies (unscaled and scaled) calculated at HF and B3LYP levels using the triple split valence basis set along with the diffuse and polarization functions, 6-311++G(d,p) and observed FT-IR and FT-Raman frequencies for various modes

of vibrations have been presented in Table 2. The experimental and theoretical FTIR and FT-Raman spectra are shown in Figures. 2 and 3. The functional group frequencies of various bonds are discussed below.

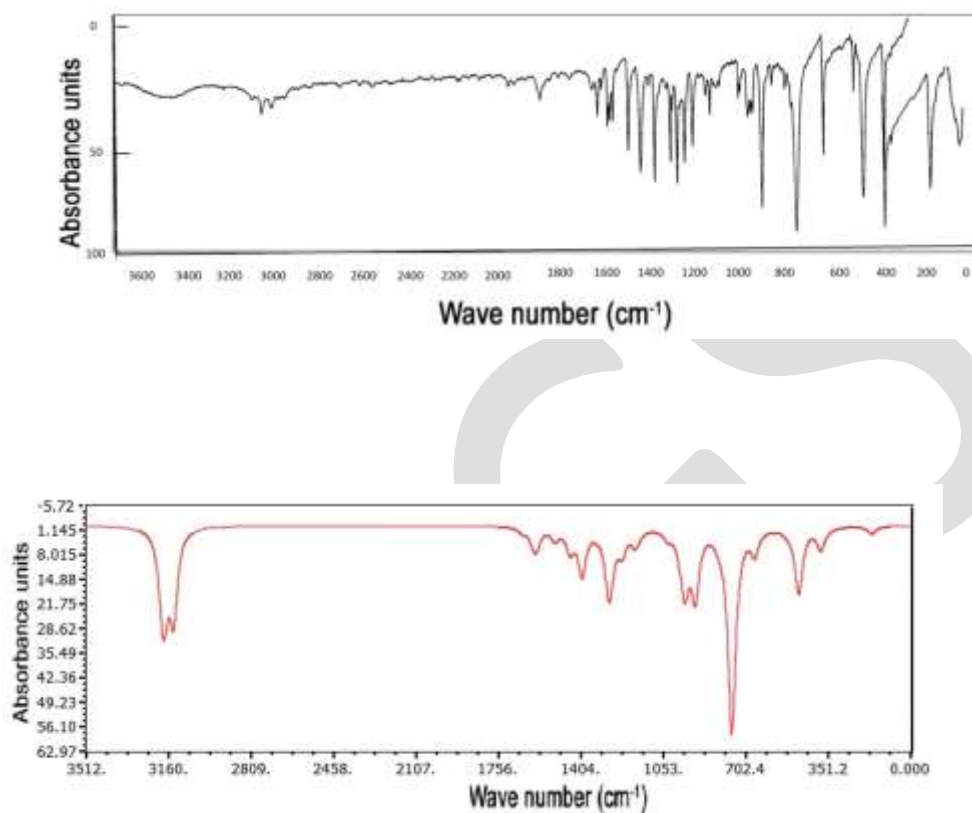
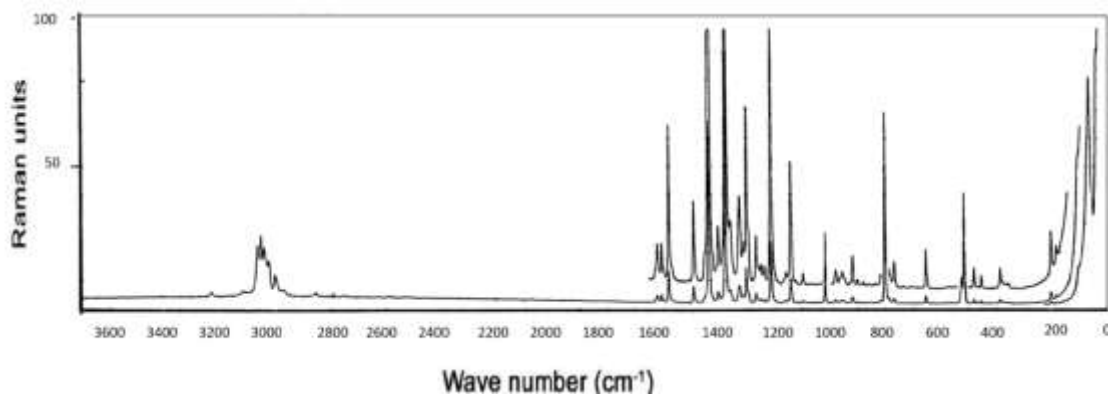


Figure 2: Experimental (top) and theoretical (bottom) FTIR spectra of Phthalazine.



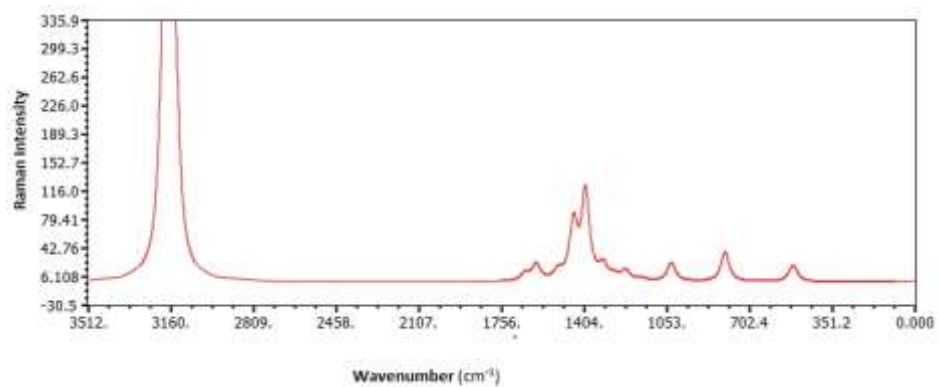


Figure 3: Experimental (top) and theoretical (bottom) FT-Raman spectra of Phthalazine.

S.no	Experimental		B3LYP/6-311++G** Calculated wavenumber		IR intensity	Raman Activity	HF/6-311++G** Calculated wavenumber		IR intensity	RamanA ctivity	Assignment
	IR	Rama n	unscaled	scaled			unscale d	scale d			
1		178	168	157	2.197	0.314	186	178	1.960	0.319	Ring deformation
2	181	198	173	173	0	0.001	195	195	0	0.012	γ CC+ γ C-C-C
3	353	350	354	354	0.397	0.017	378	359	0.383	0.013	γ N-C-C
4	360	382	386	382	5.975	0.335					C-C-C and C-N-C
5		450	451	451	0	0.004	435	435	4.295	1.037	γ C-C-C + β NCC
6	473	476	480	480	18.290	0.043	493	478	0	0.228	γ C-C-C
7	515		516	516	0.393	14.144	534	517	26.657	0.001	β CCC+ γ CCH+ γ NCC
8		522	528	522	0.653	8.098	546	524	0.511	9.362	β C-C-C + γ CNC + γ NCC
9		570					564	564	0.718	7.315	β CCC+ β CC+ β CCH+ β CN
10	622		646	626	0	0.247	694	652	0	0.132	γ C-C-C
11	645	651	668	654	6.570	1.586	710	667	8.845	1.426	γ C-C-C + ν CH
12	761	761	765	765	57.251	0.038	811	770	0	0.623	β C-C-C + ν_s CH +RING BREATHING
13	791	781	781	781	0	0.252	842	791	70.903	0.132	γ CH +CCC RING BREATHING+HN CC
14		797	810	793	0.797	37.781					ν_s CH + ν_s CN
15	816	811	822	813	1.546	0.227	867	814	1.841	29.745	CH ν_s +CC RING BREATHING
231 16	868	878	879	879	0	www.ijergs.org 0.006	872	837	3.626	0.316	CCC RING BREATHING + γ CH

17	953	946	921	912	18.380	0.105	964	954	0	0.186	γ CH + β CN
18	969	972	946	946	0	0.349	1042	1010	2.229	0.073	β CCC+ γ CH
19	1017		964	964	13.912	0.073	1024	1013	17.728	0.923	γ CH
20	1008	1013	971	971	1.885	0.005	1048	1006	0	0.060	β CH
21	1034		983	973	3.432	0.207	1040	1040	19.595	4.329	β CCC + v_s CH
22		1089	1008	1008	0	0.071	1102	1090	0.041	17.317	β CCC + γ CC +RING DEFORMATION
23	1095	1135	1038	1038	2.294	23.807	1097	1094	3.216	0.857	v N-N +CCC TRIGONAL BEND
24	1137		1160	1136	0.957	2.674	1118	1097	0	0.668	β CH + β CCC
25		1156	1177	1153	4.227	1.510					v_s C=C + v_s CN
26	1208	1213	1232	1207	6.252	13.246	1221	1221	8.448	1.691	β CH + v_s CN
27	1244	1229	1278	1239	4.815	4.149	1243	1243	0.552	3.550	β CH + v_s C=C
28	1237	1259	1289	1237	16.075	2.356					v_s C-C
29	1277	1294	1328	1258	0.909	0.821					v_s CC
30	1302		1339	1301	0.001	17.275					γ CC+ γ CN+ β CCN
31	1322	1318					1301	1318	1.889	9.909	v CN
32	1370	1351					1367	1367	15.703	2.199	v_s CC
33	1400	1378					1378	1378	4.427	2.865	v CN+ v_s CC
34	1432	1396	1403	1403	12.938	113.464	1444	1429	11.479	55.260	v_s CC
35	1451	1437	1453	1438	5.656	69.15	1461	1431	2.974	3.279	v_s CC + v_s CN
36		1483	1464	1464	0.595	2.732					v_s CC
37	1487		1519	1488	3.306	10.866	1498	1483	7.121	147.524	v_s C=C
38	1532						1587	1539	11.276	95.543	v CC
39	1555	1575	1598	1582	5.356	0.510	1587	1555	0.322	0.193	C=C v_s + v CC
40	1601	1610	1613	1613	2.648	20.773	1646	1613	7.441	19.379	v_s C=C
41	1646	1618	1659	1642	1.326	9.664					v_s C=C + v_s C-C
42	1740						1775	1739	11.458	0.831	v CC+ β HCC

43		1788					1783	1783	1.901	35.034	v RING+ v CC+β HCC
44	1869						1829	1829	0.431	3.150	v RING
45	2968	2784	3143	2985	23.505	18.465					v _{as} CH
46		3014	3145	3019	0.420	204.529					v _s CH
47	3026	3090	3167	3090	0.674	25.707					v _s CH
48		3143	3172	3162	0.774	135.782					v _s CH
49	3068		3183	3055	16.728	59.697	3320	3120	20.448	9.837	v _{as} CH
50		3123	3193	3129	11.877	305.432					v _{as} CH
51		3227					3322	3211	0.855	123.563	v _{as} CH
52	3230						3325	3222	1.795	43.672	v _{as} CH
53		3300					3333	3227	2.714	146.144	v _{as} CH
54	3470						3345	3233	22.447	38.157	v _{as} CH
55	3674						3355	3355	13.568	263.702	v _{as} CH

Table 2: Experimental and calculated (B3LYP/6-311++G(d,p) and HF/6-311++G(d,p) levels) vibrational frequencies (cm⁻¹), IR Intensity (KM Mol⁻¹), Raman Activity (Å⁴amu⁻¹) of Phthalazine.

N- N vibrations:

The N-N stretching mode is reported at 1093 cm⁻¹ experimentally for Phthalazine derivatives [35]. In our present study the N-N stretching vibrations are observed at 1095 cm⁻¹ in FTIR and the theoretically computed N-N vibrations in the region 1098 cm⁻¹ by HF method show good agreement with experimental value.

C-N Vibrations:

The identification of C-N vibrations is a very difficult task since mixing of several bands is possible in this region. However, from the help theoretical calculations, the v C-N vibrations are identified and assigned in this study. Silverstein et al., assigned the C-N stretching vibrations in the region 1382–1266 cm⁻¹ for aromatic amines [36]. The frequencies 1598- 1411 cm⁻¹ in both FT-IR and FT-Raman spectra have been assigned to C-N, C=N stretching vibration, respectively [37]. Referring the previous reference the band at 1598-1468 cm⁻¹, has been designed to C-N stretching mode. Hence in the present investigation, the symmetric CN vibrations are

observed FTIR in 1208,1322,1400 and 1451 cm^{-1} and in Raman it is observed at 797,1156,1213,1318,1378 and 1437 cm^{-1} Whereas its corresponding calculated scaled values are 793,1153,1207 and 1438 in DFT method and 1221,1318 and 1378 cm^{-1} in HF method. The in plane bending vibrations of C-N bending in found in 953 cm^{-1} in IR and 946 cm^{-1} in raman spectrum.

C-C /C=C vibrations:

The ring carbon-carbon stretching vibrations usually occur in the region 1600–1400 cm^{-1} [38,39]. The ring carbon-carbon stretching vibrations in benzene ring occur in the region 1625-1430 cm^{-1} . For aromatic six-membered rings, e.g., benzene and pyridines, there are two or three bands in this region due to skeletal vibrations, the strongest usually being at about 1500 cm^{-1} . In the case where the ring is conjugated further a band at about 1580 cm^{-1} is also observed [38]. The symmetric C-C stretching vibrations are observed at Socrates

[38] mentioned that the presence of conjugate substituent such as C=C causes a heavy doublet formation around the region 1625-1575 cm^{-1} . In the present work the symmetric C-C stretching vibrations are found in

1244,1237,1277,1370,1400,1432,1451,1535,1555,1740 cm^{-1} in FTIR. In

1259,1294,1351,1396,1351,1396,1437,1483,1575,1788 cm^{-1} in Raman spectrum. Likewise the symmetric C=C stretching vibrations are found in 1244,1601 in FTIR and in 1156,1229,1610 cm^{-1} in Raman spectrum. Out of plane bending vibrations of C-C are observed at 1089 cm^{-1} in Raman and at 1302 cm^{-1} in FTIR spectrum. The bands occurring at 515,622,645,761,969,1034 and 1137 cm^{-1} in the infrared and at 522,570,651,761,781,878,972 and 1089 cm^{-1} in Raman spectrum are assigned to the in plane bending CCC in-plane bending modes of Phthalazine.

C-H vibrations:

Aromatic compounds commonly exhibit multiple weak bands in the region 3100–3000 cm^{-1} [40] due to aromatic C-H stretching vibrations. All the C-H stretching vibrations are very weak in intensity. The bands due to C-H in-plane bending vibrations are observed in the region 1390–990 cm^{-1} [41]. The bands due to the C-H in-plane deformation vibrations, which usually occurs in this region are very useful for characterization and are very strong indeed [42]. When there is in-plane interaction above 1200 cm^{-1} , a carbon and its hydrogen usually move in opposite direction [43]. The out of plane C-H vibrations are strongly coupled and occur in the region of 1000–700 cm^{-1} [44]. In our present Phthalazine molecule the symmetric and asymmetric C-H stretching vibrations are found in between 3026- 3674 cm^{-1} in FTIR spectrum and also it appears in Raman spectrum it is in between 3014-3300 cm^{-1} which shows the correlation with the literature survey. The in plane bending vibrations of C-H are verified at 1008,1095,1137,1208,1244 cm^{-1} in FTIR and at 1013,1135,1213 and 1229 cm^{-1} in Raman spectrum. The out of plane bending vibrations are found in 645,761,791 and 969 cm^{-1}

in FTIR and at 651,761,781,878 and 972 cm^{-1} in Raman spectrum. For most of the remaining ring vibrations, the overall assignments are satisfactory. Small changes in frequencies observed for these modes are due to the changes in force constants or reduced mass ratio resulting mainly due to the extent of mixing between ring and substituent.

3.3 Non linear optical effects:

NLO effects arise from the interactions of electromagnetic fields in various media to produce new fields altered in phase, frequency, amplitude or other propagation characteristics from the incident fields [45]. NLO is at the forefront of current research because of its importance in providing the key functions of frequency shifting, optical modulation, optical switching, optical logic, and optical memory for the emerging technologies in areas such as telecommunications, signal processing, and optical interconnections [46-49].

Dipole moment, polarizability and hyperpolarizabilities of organic molecules are important response properties. There has been an intense investigation for molecules with large non-zero hyperpolarizabilities, since these substances have potential as the constituents of non-linear optical materials. In presence of an applied electric field, the energy of a system is a function of the electric field. The first hyper polarizability is a third-rank tensor that can be described by a $3 \times 3 \times 3$ matrix. The 27 components of the 30 matrix can be reduced to 10 components due to the Kleinman symmetry[50]. The components of β_0 are defined as the coefficients in the Taylor series exponents the energy in the external electric field. When the external electric field is weak and homogeneous, this expansion becomes

$$E=E^0-\mu_a F_a - 1/2\alpha_{a\beta} F_a F_\beta - 1/6\beta_{a\beta\gamma} F_a F_\beta F_\gamma + \dots$$

where E^0 is the energy of the unperturbed molecules, F_a is the field at the origin and μ_a , $\alpha_{a\beta}$ and $\beta_{a\beta\gamma}$ are the components of dipole moment, polarizability and the first-order hyperpolarizabilities respectively.

In present study, the electronic dipole moment, molecular polarizability, anisotropy of polarizability and molecular first hyperpolarizability of present compound were investigated. The polarizability and hyperpolarizability tensors [α_{xx} , α_{xy} , α_{yy} , α_{xz} , α_{yz} , α_{zz} and β_{xxx} , β_{xyy} , β_{yyy} , β_{xxz} , β_{xyz} , β_{yyz} , β_{xzz} , β_{yzz} , β_{zzz}] can be obtained by a frequency job output file of Gaussian. The total static dipole moment (μ), the mean polarizability(α_0), the anisotropy of the polarizability (Δ_a) and the mean first-order hyperpolarizability (β_0), using the x, y, z components they are defined as follows:

$$\alpha_{\text{total}} = \alpha_0 = 1/3 (\alpha_{xx} + \alpha_{yy} + \alpha_{zz})$$

$$\Delta\alpha = [(\alpha_{xx} - \alpha_{yy})^2 + (\alpha_{yy} - \alpha_{zz})^2 + (\alpha_{zz} - \alpha_{xx})^2 + 6\alpha_{xz}^2 + 6\alpha_{xy}^2 + 6\alpha_{yz}^2]^{1/2}$$

$$\beta_0 = (\beta_x^2 + \beta_y^2 + \beta_z^2)^{1/2}$$

$$= [(\beta_{xxx} + \beta_{xyy} + \beta_{xzz})^2 + (\beta_{yyy} + \beta_{xxy} + \beta_{yzz})^2 + (\beta_{zzz} + \beta_{xxz} + \beta_{yyz})^2]^{1/2}$$

$$\Delta\alpha = [(\alpha_{xx} - \alpha_{yy})^2 + (\alpha_{yy} - \alpha_{zz})^2 + (\alpha_{zz} - \alpha_{xx})^2 / 2]^{1/2}$$

The α and β values of the Gaussian 05 output are in atomic units (a.u) and these calculated values converted into electrostatic unit (e.s.u) ($\alpha : 1 \text{ a.u} = 0.1482 \times 10^{-24} \text{ esu}$; for $\beta : 1 \text{ a.u} = 8.639 \times 10^{-33} \text{ esu}$;) and these above polarizability values of Phthalazine are listed in Table (3). The total dipole moment can be calculated using the following equation.

$$\mu = (\mu_x^2 + \mu_y^2 + \mu_z^2)^{1/2}$$

To study the NLO properties of molecule the value of urea which is prototypical molecule is used as threshold value for the purpose of comparison. Urea is the prototypical molecule used in the study of the NLO properties of the molecular systems.

The total molecular dipole moment and first order hyperpolarizability are 5.3032 Debye and $0.2496831305 \times 10^{-30} \text{ cm}^5/\text{esu}$, respectively and are depicted in Table 3. Total dipole moment of title molecule is approximately four times greater than that of urea and first order hyperpolarizability is 0.1 times lesser than that of urea (μ and β of urea are 1.3732 Debye and $0.3728 \times 10^{-30} \text{ cm}^5/\text{esu}$ obtained by HF/6-311G(d,p) method [51]. These results indicate that the title compound is a good candidate of NLO material.

Parameters (a.u)	DFT B3LYP/6-311++G(d,p)	HF /6-311++G(d,p)
α_{xx}	54.7857473	131.520057
α_{xy}	-0.000000489249679	0.00000000759618116
α_{yy}	145.958031	103.675498
α_{xz}	0.0000000000379414449	-0.0000000549565194
α_{yz}	0.0000000217153642	0.0000000266667497
α_{zz}	111.953395	53.9545493
α_0	104.2323911	96.3833681

$\Delta\alpha$	79.80161726	68.0577788
β_{xxx}	-0.00000248429697	-41.8501250
β_{xxy}	52.0398273	-0.000000430891865
β_{xyy}	0.00000357237014	15.2046515
β_{yyy}	-82.2554657	0.000000224286613
β_{xxz}	0.0000000197723763	-0.00000154879012
β_{xyz}	-0.000000163513452	0.000000761285762
β_{yyz}	0.00000170415196	-0.00000227357450
β_{xzz}	0.00000381123329	55.5473291
β_{yzz}	-4.10579237	-0.0000000703065283
β_{zzz}	0.00000000865477438	-0.000000886088144
β	34.32143077 a.u	28.9018556a.u
	$2.965028404 \times 10^{-31}$	$2.496831305 \times 10^{-31}$
μ_x	-5.3032	5.4630
μ_y	0.0000	0.0000
μ_z	0.0000	0.0000
μ total (Debye)	5.3032	5.4630

Table 3: The electric dipole moment, polarizability and first order hyperpolarizability of

Phthalazine.

The theoretical calculation of β components is very useful as this clearly indicates the direction of charge delocalization. In β_{xzz} direction, the biggest values of hyperpolarizability are noticed and subsequently delocalization of electron cloud is more in that direction. The maximum β value may be due to π electron cloud movement from donor to acceptor which makes the molecule highly polarized and the intra molecular charge transfer possible.

3.4 Frontier molecular orbital analysis:

To understand this phenomenon in the context of molecular orbital theory, we examined the molecular HOMOs and molecular LUMOs of the title compound. When we see the first hyperpolarizability value, there is an inverse relationship between first hyperpolarizability and HOMO–LUMO gap, allowing the molecular orbitals to overlap to have a proper electronic communication conjugation, which is a marker of the intra molecular charge transfer from the electron donating group through the p-conjugation system to the electron accepting group [52,53].

The total energy, energy gap and dipole moment affect the stability of a molecule. Surfaces for the frontier orbital were drawn to understand the bonding scheme of present compound and it is shown in Figure 4. The Frontier orbital gap helps to characterize the chemical reactivity kinetic stability, chemical reactivity, optical polarizability, chemical hardness, softness of a molecule [54].

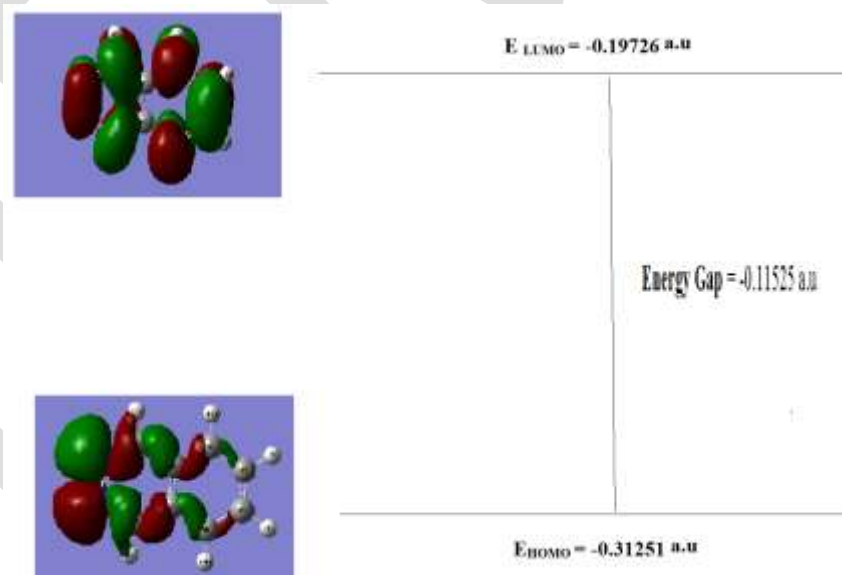


Figure 4: Patterns of the principle highest occupied and lowest unoccupied molecular orbitals of Phthalazine.

The highest occupied molecular orbital (HOMO) and the lowest unoccupied molecular orbital (LUMO) are known as frontier molecular orbitals (FMOs). The HOMO is the orbital that primarily acts as an electron donor and the LUMO is the orbital that largely acts as the electron acceptor, and the gap between HOMO and LUMO characterizes the molecular chemical stability. The energy gap between the HOMO and the LUMO molecular orbitals is a critical parameter in determining molecular electrical transport properties because it is a measure of electron conductivity. The chemical activity of the molecule is also observed from eigen values of LUMO and HOMO and from the energy gap value calculated from them. (HOMO–LUMO) separation, which is the result of a significant degree of intermolecular charge transfer (ICT) from the endcapping electron-donor to the efficient electron acceptor group through p-conjugated path. [55, 56].

The computed energy values of HOMO and LUMO in gas phase are -0.31251 eV and -0.19726 eV respectively. The energy gap value is -0.11525 eV for Phthalazine molecule. The energy values of the frontier orbitals are presented in Table 4. By using HOMO and LUMO energy values for a molecule, the ionization potential and chemical hardness of the molecule were calculated using Koopmans' theorem [57] and are given by $\eta = (I_P - E_A)/2$ where $I_P \sim E(\text{HOMO})$, $E_A \sim E(\text{LUMO})$, I_P = Ionization potential (eV), E_A = electron affinity (eV)

$$\eta = \frac{1}{2} (\epsilon_{\text{LUMO}} - \epsilon_{\text{HOMO}}).$$

The hardness has been associated with the stability of chemical system. Considering the chemical hardness, large HOMO–LUMO gap means a hard molecule and small HOMO–LUMO gap means a soft molecule. One can also relate the stability of molecule to hardness, which means that the molecule with least HOMO–LUMO gap means it is more reactive. The electron affinity can be used in combination with ionization energy to give electronic chemical potential, $\mu = \frac{1}{2} (\epsilon_{\text{LUMO}} + \epsilon_{\text{HOMO}})$. Chemical softness (S) = $1/\eta$ describes the capacity of an atom or group of atoms to receive electrons and is the inverse of the global hardness [58]. The soft molecules are more polarizable than the hard ones because they need small energy to excitation. A molecule with a low energy gap is more polarizable and is generally associated with the high chemical activity and low kinetic stability and is termed soft molecule [59]. A hard molecule has a large energy gap and a soft molecule has a small energy gap [60]. It is shown from the calculations that Phthalazine has the least value of global hardness (0.057625eV) and the highest value of global softness (17.353579 eV) is expected to have the highest inhibition efficiency. The global electrophilicity index, $\omega = \mu^2/2\eta$ is also calculated and these values are listed in Table 4.

Molecular properties	DFT-B3LYP/6-311++G(d,p)
E_{LUMO+1} (eV)	-0.17640
E_{LUMO} (eV)	-0.19726
E_{HOMO} (eV)	-0.31251
E_{HOMO-1} (eV)	-0.33801
$\Delta E_{HOMO-LUMO}$ (eV)	-0.11525
$\Delta E_{HOMO-LUMO+1}$ (eV)	-0.13611
$\Delta E_{HOMO-1-LUMO}$ (eV)	-0.14075
$\Delta E_{HOMO-1-LUMO+1}$ (eV)	-0.16161
Global hardness(η)	0.057625
Chemical softness(S)	17.353579
Electronic chemical potential(μ)	0.254885
Global electrophilicity index(ω)	0.5636994

Table 4: Calculated energy values of Phthalazine in its ground state.

3.5 Mullikan analysis:

In the application of quantum mechanical calculations to molecular system, the calculation of effective atomic charges plays an important role. The results are given in Table 5. The magnitude of two nitrogen atoms is 0. The carbon atomic charges found to be either positive or negative, were noted to change from -0.1 to 1.11. All the hydrogen atoms have positive values.

S.NO	ATOMS	B3LYP/6-	HF

		311++G(d,p)	
1	1N	0.000758	-0.02334
2	2N	0.000758	-0.02334
3	3C	-0.5852	-0.60769
4	4C	1.118006	1.115744
5	5C	-0.8961	-0.96304
6	6C	-0.1654	-0.143
7	7C	-0.1654	-0.143
8	8C	-0.8961	-0.96304
9	9C	1.118006	1.115744
10	10C	-0.5852	-0.60769
11	11H	0.20307	0.228608
12	12H	0.150086	0.181445
13	13H	0.17478	0.211277
14	14H	0.17478	0.211277
15	15H	0.150086	0.181445
16	16H	0.20307	0.228608

Table 5: Mulliken atomic charges of Phthalazine for B3LYP and HF with 6-311++G(d,p) basis sets.

3.6 Thermodynamic properties:

The values of some thermodynamic parameters (such as zero point vibrational energy, thermal energy, specific heat capacity, rotational constants, rotational temperature) of title molecule by DFT/B3LYP/6-311++G(d,p) and HF/ B3LYP/6-311++G(d,p) methods are listed in Table 6. On the basis of vibrational analysis, These parameters are listed out based on the statistically thermodynamic functions : heat capacity(C), enthalpy changes(H) and entropy (S) for the title compound. Here, all thermodynamic calculations were done in gas phase and listed in Table 6.

Parameters	B3LYP/6-311++G(d,p)	HF
Dipole moment (Debye)	5.3032	5.4630
Zero point energy	321641.8 (Joules/Mol) 76.87424 (Kcal/Mol)	345011.5 (Joules/Mol) 82.45973 (Kcal/Mol)
Entropy (Cal/Mol-Kelvin)		
Total	81.877	80.108
Translational	40.501	40.501
Rotational	28.871	28.826
Vibrational	12.504	10.781
Rotational temperature (Kelvin)		
	0.15705	0.15963
	0.05938	0.06024
	0.04309	0.04374
Rotational constants (GHZ)		
	3.27233	3.32623
	1.23722	1.25524

	0.89778	0.91133
Thermal Energy (KCal/Mol)		
Total	81.081	86.358
Translational	0.889	0.889
Rotational	0.889	0.889
Vibrational	79.304	84.581
Molar capacity at constant volume (Cal/Mol-Kelvin)		
Total	27.391	25.057
Translational	2.981	2.981
Rotational	2.981	2.981
Vibrational	21.430	19.096

Table 6 : Theoretically computed Dipole moment(Debye), energy(au), zero point vibrational energy(kcal mol⁻¹), entropy(cal mol⁻¹k⁻¹), rotational temperature(Kelvin), rotational constant(GHz), thermal energy(Kcal/Mol) and Molar capacity at constant volume(Cal/Mol-Kelvin)of Phthalazine.

3.7 ¹H NMR analysis

The NMR experimental and theoretical chemical shifts are used to identify the organic compounds and ionic species. It is recognized that accurate predictions of optimized molecular geometrics are essential for reliable calculations of magnetic properties [61]. GIAO(Gauge –Including Atomic Orbital) procedure is somewhat superior since it exhibits a faster convergence of the calculated properties upon extension of the basis set used. Taking into account the computational cost and the effectiveness of calculation, the GIAO method seems to be preferable from many aspects at the present state of this subject. On the other hand, the density functional

methodologies offer an effective alternative to the conventional correlated methods, due to their significantly lower computational cost.

Application of the GIAO [62] approach to molecular systems was significantly improved by an efficient application of the method to the ab initio SCF calculations, using techniques borrowed from analytic derivative methodologies. GIAO method is one of the most common approaches for calculating isotropic nuclear magnetic shielding tensors. [63] ^1H NMR chemical shifts calculations of the title compounds have been carried out by using B3LYP functional with 6-311G++(d,p) basis set. The NMR spectra calculations were performed by using the Gaussian03 program package. Experimental and theoretical chemical shifts of Phthalazine in ^1H NMR spectra were recorded and the obtained data are presented in Table 7. The combined use of Experimental NMR and computer simulation methods offers a powerful way to interpret and predict the structure of large biomolecules. The theoretical and experimental ^1H and NMR spectra are shown in Figure 5.

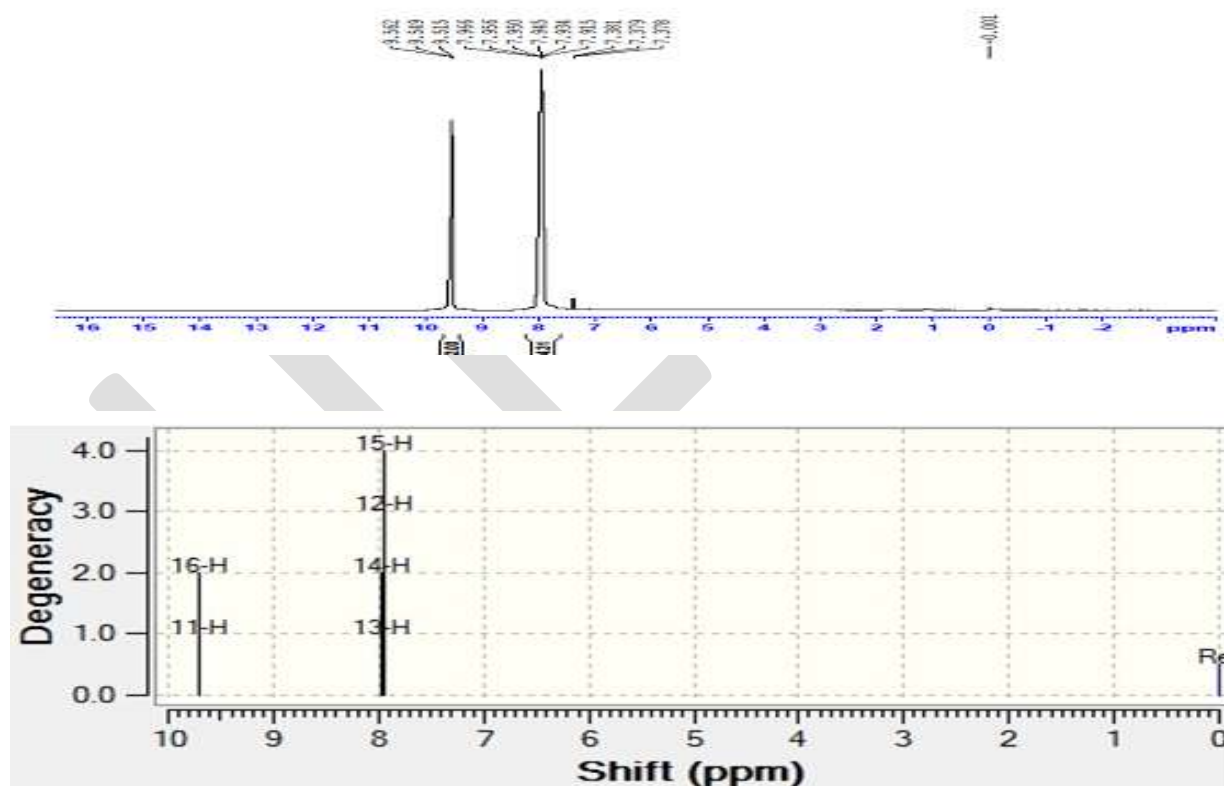


Figure 5: Experimental (upper) and Theoretical(bottom) ^1H NMR spectrum of Phthalazine.

S.NO	ATOMS	Experimental Chemical shift)	Calculated chemical shift by B3LYP method
1	11H	9.562	9.696
2	12H	7.966	7.953
3	13H	7.956	7.953
4	14H	7.950	7.953
5	15H	7.945	7.953
6	16H	9.549	9.696

Table 7: The observed (in CDCl₃) and predicted ¹H NMR isotropic chemical shifts (with respect to TMS, all values in ppm) for Phthalazine.

3.8 UV spectrum and electronic properties:

The lowest singlet- singlet spin-allowed excited states were taken into account for the TD-DFT calculation in order to investigate the properties of electronic absorption of Phthalazine molecule. The energies of four important molecular orbitals of Phthalazine : the second highest and highest occupied MO's (HOMO and HOMO-1), the lowest and the second lowest unoccupied MO's (LUMO and LUMO + 1) were calculated and are presented in Table 4. The experimental λ_{\max} values are obtained from the UV/Visible spectra recorded in CHCl₃. The Figure.6. depicts the observed and the theoretical UV-Visible spectra of Phthalazine. The calculations were also performed with CHCl₃ solvent effect. The calculated absorption wavelengths (λ_{\max}) and the experimental wavelengths are also given in Table 8.

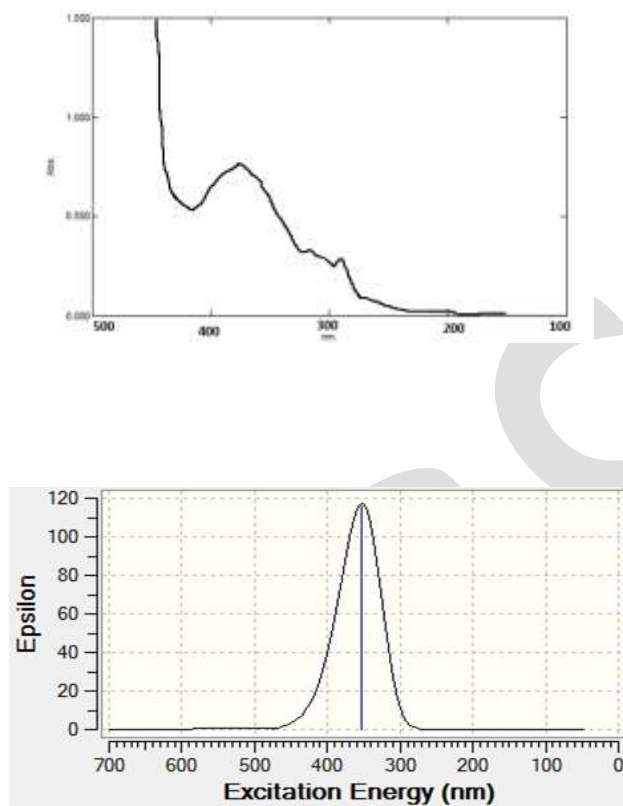


Figure 6: Experimental UV spectra of Phthalazine.

In the electronic absorption spectrum of Phthalazine, there are three absorption bands with a maximum **390.60,357.20,291.00** nm. The strong absorption band **357.20** nm is caused by the $n \rightarrow \pi^*$ [64,65] and the other two moderately intense bands are due to $\pi \rightarrow \pi^*$ transitions [66,67]. The $\pi \rightarrow \pi^*$ transitions are expected to occur relatively at lower wavelength, due to the consequence of the extended aromaticity of the ring and high energy transitions.

Then in Phthalazine molecule the $n \rightarrow \pi^*$ transition is more significant due to the presence of lone pair of electrons in the nitrogen atoms. The 3D plots of important molecular orbitals are shown in Figure. 4. The energy gap between HOMO and LUMO is a critical parameter in determining molecular electrical transport properties [68].The energy gap of HOMO–LUMO explains the eventual charge transfer interaction within the molecule, and the frontier orbital energy gap in case of Phthalazine is found to be 0.11525 eV obtained at TD-DFT method using 6-311++G(d,p) basis set.

Experimental		STATES	Calculated by B3LYP/6-311++G(d,p)		
λ (nm)	Log (ϵ)		λ (nm)	E (eV)	(f)
390.60	0.005	34 -> 35	475.01	2.6101	0.0000
357.20	0.011	34 -> 36	352.63	3.5160	0.0029
291.00	0.328	34 -> 35 34 -> 37	271.77	4.5620	0.0000

Table 8: Theoretical electronic absorption spectra of Phthalazine (absorption wavelength λ (nm), excitation energies E (eV) and oscillator strengths (f) using TDDFT/B3LYP/6-311++G(d,p) method in gas phase.

4. CONCLUSION

In this study, we attempted to clarify the characterization of Phthalazine by means of both experimental and computational methods. Bond lengths and angles were calculated by using DFT and HF methods and compared with each other. All compared data were shown to have in a good agreement with each other. The non linear optical property of the compound also calculated with the hyperpolarizability values. Moreover, after frontier molecular orbitals and electronic structure, energy band gap and Mullikan charges of the title molecule were investigated and interpreted. Atomic charges, thermodynamic properties, NMR spectra and UV-Vis spectra were also determined for the identification of the molecule. Theoretical ¹H chemical shifts were found to be in good agreement with the experimental determines. In conclusion, all the calculated data and simulations not only show the way to the characterization of the molecule but also help for the application in Pharmaceutical industries and fundamental researches in chemistry and biology in the future.

REFERENCES:

1. Al'-Assar, F.; Zelenin, K. N.; Lesiovskaya, E. E.; Bezant, I. P.; Chakchir, B. A. *Pharm. Chem. J.* **2002**, *36*, 598-603.
2. Carling, R. W.; Moore, K. W.; Street, L. J.; Wild, D.; Isted, C.; Leeson, P. D.; Thomas, S.; O'Connor, D.; McKernan, R. M.; Quirk, K.; Cook, S. M.; Atack, J. R.; Wafford, K. A.; Thompson, S. A.; Dawson, G. R.; Ferris, P.; Castro, J. L. *J. Med. Chem.* **2004**, *47*, 1807-1822.
3. Jain, R. P.; Vederas, J. C. *Bioorg. Med. Chem. Lett.* **2004**, *14*, 3655-3658.
4. Chorghade, M. S. In *Drug Discovery and Development*; John Wiley & Sons: Hoboken, New Jersey, **2007**; Vol. 2.
5. Lednicer, D.; Mitscher, L. A. In *The Organic Chemistry of Drug Synthesis*; John Wiley & Sons: New York, Chichester, Brisbane, Toronto, **1977**; Vol. 1.
6. Grasso, S.; De Sarro, G.; De Sarro, A.; Micale, N.; Zappala, M.; Puia, G.; Baraldi, M.; De Micheli, C. *J. Med. Chem.* **2000**, *43*, 2851-2859.
7. Nomoto, Y.; Obase, H.; Takai, H.; Teranishi, M.; Nakamura, J.; Kubo, K. *Chem. Pharm. Bull.* **1990**, *38*, 2179-2183
8. Cardia, M. C.; Distinto, E.; Maccioni, E.; Delogu, A. *J. Heterocycl. Chem.* **2003**, *40*, 1011.
9. Cockcroft, X.; Dillon, K. J.; Dixon, L.; Drzewiecki, J.; Eversley, P.; Gomes, S.; Hoare, J.; Kirrigan, F.; Natthews, I.; Menear, K. A.; Martin, N. M. B.; Newton, R.; Paul, J.; Smith, G. C. M.; Vile, J.; Whittlr, A. *J. Bioorg. Med. Chem. Lett.* **2006**, *16*, 1040-1044.
10. Cockcroft, X.; Dillon, K. J.; Dixon, L.; Drzewiecki, J.; Kirrigan, F.; Loh, V. M.; Martin, N. M. B.; Menear, K. A.; Smith, G. C. M. *Bioorg. Med. Chem. Lett.* **2005**, *15*, 2235-2239.
11. Kim, J. S.; Lee, H.; Suh, M.; Choo, H. P.; Lee, S. K.; Park, H. J.; Kim, C.; Park, S. W.; Lee, C. *Bioorg. Med. Chem.* **2004**, *12*, 3683-3686.
12. Haikal, A.; El-Ashery, E.; Banoub, J. *Carbohydr. Res.* **2003**, *338*, 2291-2299.
13. Demirayak, S.; Karaburun, A.; Beis, R. *Eur. J. Med. Chem.* **2004**, *39*, 1089-1095.
14. Watanabe, N.; Kabasawa, Y.; Takase, Y.; Matsukura, M.; Miyazaki, K.; Ishihara, H.; Kodama, K.; Adashi, H. *J. Med. Chem.* **1998**, *41*, 3367-3372.
15. Johnsen, M.; Rehse, K.; Petz, H.; Stasch, J.; Bischoff, E. *Arch. Pharmacol.* **2003**, *336*, 591-597.
16. Madhavan, G. R.; Chakrabarti, R.; Kumar, S. K.; Misra, P.; Mamidi, R. N.; Balraju, V.; Ksiram, K.; Babu, R. K.; Suresh, J.; Lohray, B. B.; Lohray, V. B.; Iqbal, J.; Rajagopalan, R. *Eur. J. Med. Chem.* **2001**, *36*, 627-637.

17. Lenz, E. M.; Wilson, I. D.; Wright, B.; Partidge, E. A.; Roddgers, C. T.; Haycock, P. R.; Lindon, J. C.; Nicholson, J. K. *J. Pharm. Biomed. Anal.* **2002**, *28*, 31-43.,
18. Dogruer, D. S.; Kupeli, E.; Yesilada, E.; Sahin, M. F. *Arch. Pharmacol.* **2004**, *337*, 303-310.
19. Napoletano, M.; Norcini, G.; Pellacini, F.; Marchini, F.; Moraazzoni, G.; Ferlenga, P.; Pradella, L. *Bioorg. Med. Chem. Lett.* **2000**, *10*, 2235-2238.
20. Chakraborti, A. K.; Gopalakrishnan, B.; Sobhia, E.; Malde, A. *Bioorg. Med. Chem. Lett.* **2003**, *13*, 2473-2479. Van der Mey, M.; Hatzelmann, A.; Van Klink, G. P.; Van der Lann, I. J.; Sterk, G. J.; Thibaut, U.; Timmerman, H. *J. Med. Chem.* **2001**, *44*, 2511-2522.
21. Van der Mey, M.; Hildegard, B.; Dennis, C.; Hatzelmann, A.; Timmerman, H. *J. Med. Chem.* **2002**, *45*, 2526-2533.
22. Shubin, K. M.; Kuznetsov, V. A.; Galishev, V. A. *Tetrahedron Lett.* **2004**, *45*, 1407-1408.
23. del Olmo, E.; Barboza, B.; Ybarra, M. I.; Lopez-Perez, J. L.; Carron, R.; Sevilla, M. A.; Boselli, C.; Feliciano, A.S. *Bioorg. Med. Chem. Lett.* **2006**, *16*, 2786-2790.
24. Cashman, J. R.; Voelker, T.; Johnson, R.; Janowsky, A. *Bioorg. Med. Chem.* **2009**, *17*, 337-343.
25. D.C. Young, *Computational Chemistry: A Practical Guide for Applying Techniques to Real World Problems* (Electronic), John Wiley & Sons Inc., New York, **2001**.
26. M. Karabacak, A. Coruh, M. Kurt, *J. Mol. Struct.* **892** (2008) 125-131
27. Sundaraganesan, S. Illakiamani, H. Saleem, P.M. Wojciechowski, D. Michalska, *Spectrochim. Acta* **61A** (2005) 2995.
28. T. Prabhu, S. Periandy, S. Ramalingam, *Spectrochim. Acta* **83** (2011) 8-16.
29. M.J. Frisch, J.A. Pople, J.S. Binkley, *J. Chem. Phys.* **80** (1984) 3265-3269.
30. R. Ditchfield, *Mol. Phys.* **27** (1974) 789-807
31. M.J. Frisch et al., *Gaussian 03 Program*, Gaussian, Inc., Wallingford, CT, **2004**.
32. G. Keresztury, S. Holly, J. Varga, G. Besenyi, A.Y. Wang, J.R. Durig, *Spectrochim. Acta* **9A** (1993) 2007-2026.
33. G. Keresztury, in: J.M. Chalmers, P.R. Griffith (Eds.), *Raman Spectroscopy: Theory, Hand book of Vibrational Spectroscopy*, vol. 1, John Wiley & Sons, Ltd., New York, **2002**.
34. M.J. Frisch et al., *Gaussian 09, Revision A.1*, Gaussian, Inc., Wallingford CT, **2009**.
35. Panicker, C. Y.; Ambujakshan, K. R.; Varghese, H. T.; Mathew, S.; Ganguli, S.; Nanda, A. K.; Van Alsenoy, C. J. *Raman Spectrosc.* **2009**, *40*, 527-536

36. M. Silverstein, G. Clayton Basseler, C. Morill, *Spectrometric Identification of Organic Compounds*, Wiley, New York, **1981.**,
37. N. Sundaraganesan, K. Satheshkumar, C. Meganathan, B.D. Joshua, *Spectrochim. Acta A* 65 (**2006**) 1186-1196.
38. G. Socrates, *Infrared and Raman Characteristic Group Frequencies e Tables and Charts*, third ed., *John Wiley & Sons*, Chichester, **2001.**
39. S. Jeyavijayan, M. Arivazhagan, *Indian J. Pure Appl. Phys.* 48 (**2010**) 869-874.
40. V. Krishnakumar, R.J. Xavier, *Indian J. Pure Appl. Phys.* 41 (**2003**) 597
41. A. Srivastava, V.B. Singh, *Indian J. Pure. Appl. Phys* 45 (**2007**) 714–720.
42. E.B. Wilson, J.C. Decius, P.C. Cross, *Molecular Vibrations*, *McGraw Hill*, **1978.**
43. J. Mohan, *Organic Spectroscopy – Principles and Applications*, second ed., Narosa Publishing House, New Delhi, **2001.**
44. N.P.G. Roeges, *A Guide to the Complete Interpretation of Infrared Spectra of Organic Structures*, Wiley, New York, **1994.**
45. Y.X. Sun, Q.L. Hao, W.X. Wei, Z.X. Yu, L.D. Lu, X. Wang, Y.S. Wang, *J. Mol. Struct.:Theochem.* 904 (**2009**) 74–82
46. C. Andraud, T. Brotin, Garcia, F. Pelle, P. Goldner, B. Bigot, A. Collet, *J. Am. Chem. Soc.* 116 (**1994**) 2094.
47. V.M. Geskin, C. Lambert, J.L. Bredas, *J. Am. Chem. Soc.* 125 (**2003**) 15651.
48. M. Nalano, H. Fujita, M. Takahata, K. Yamaguchi, *J. Am. Chem. Soc.* 124 (**2002**) 9648.
49. D. Sajan, I.H. Joe, V.S. Jayakumar, J. Zaleski, *J. Mol. Struct.* 785 (**2006**) 43
50. X. Sun, Q.L. Hao, W.X. Wei, Z.X. Yu, D.D. Lu Wang, Y.S. Wang, *Mol. Struct.thermo chem.* 74 (**2009**) 901–904.
51. S. Muthu, J. Uma Maheswari, *Spectrochimica Acta Part A* 92 (**2012**) 154– 163
52. M.C. Ruiz Delgado, V. Hernandez, J. Casado, J.T. Lopez Navarre, J.M. Raimundo, P. Blanchard, J. Roncali, *J. Mol. Struct.* 151 (**2003**) 651–653.
53. J.P. Abraham, D. Sajan, V. Shettigar, S.M. Dharmaprakash, I. Nemeč, I.H. Joe, V.S. Jayakumar, *J. Mol. Struct.* 917 (**2009**) 27–36.
54. D.A. Kleinman, *Phys. Rev.* 126 (**1962**) 1977–1979
55. B. Kosar, C. Albayrak, *Spectrochim. Acta* 78A (**2011**) 160–167.

56. L. Xiao-Hong, Z. Xian-Zhou, *Comput. Theor. Chem.* 963 (2011) 34–39.
57. T.A. Koopmans, *Physica I* (1934) 104–113.
58. Pearson R G, *Inorg Chem*, 1988; 27: 734-740.
59. I. Fleming, *Frontier Orbitals and Organic Chemical Reactions*, (John Wiley and Sons), NewYork, 1976
60. Obi-Egbedi N O, Obot I B, El-Khaiary M I, Umoren S A and Ebenso E E, *Int J Electro Chem Sci.*, 2011; 6:5649-5675
61. N. Subramanian, N. Sundaraganesan, J. Jayabharathi, *Spectrochim. Acta A* 76 (2010) 259.
62. R. Ditchfield, *J. Chem. Phys.* 56 (1972) 5688–5692.
63. T. Schlick, *Molecular Modeling and Simulation: An Interdisciplinary Guide, vol.21, second ed., Springer, New York, 2010.*
64. R.H. Holm, F.A. Cotton, *J. Am. Chem. Soc.* 80 (1958) 5658–5663.
65. F.A. Cotton, C.W. Wilkinson, *Advanced Inorganic Chemistry, third ed., Interscience Publisher, New York, 1972.*
66. W. Barnum, *J. Inorg. Nucl. Chem.* 21 (1961) 221–237.
67. R.M. Silverstein, G.C. Bassler, T.C. Morrill, *Spectrometric Identification of Organic Compounds, fifth ed., John Wiley & Sons, Inc., New York, 1981.*
68. K. Fukui, *Science* 218 (1982) 747